

14

Naval Ocean Research and Development Activity

November 1986

Report 126



AD-A176 365

Effects of Atmospheric Water Vapor on the Detection of Mesoscale Oceanographic Features from GEOSAT

DTIC
ELECTE
FEB 03 1987
S E D

DTIC FILE COPY

Jeffrey D. Hawkins
Peter M. Smith
Ocean Sensing and Prediction Division
Ocean Science Directorate

Executive summary

The GEOSAT Ocean Applications Program (GOAP) is using near-real-time altimeter data to map mesoscale fronts and eddies in the Gulf Stream region. This effort is hampered in part by the uncertainty introduced into the altimeter range measurement due to atmospheric water vapor attenuating the altimeter pulse, producing erroneous undulations in the resultant sea surface topography. This report identifies the magnitude and spatial scales associated with water vapor attenuation so that the GOAP analyst can better anticipate the problem at hand.

The task is approached by using SEASAT Scanning Multichannel Microwave Radiometer data to define water vapor gradients over the Gulf Stream. The 1978 data clearly reveal that attenuation due to water vapor alone can be 20-40% as large as the 50-100 cm signal characteristic of ocean fronts and eddies. These water vapor gradients also occur on the same scale (100-250 km) as the mesoscale ocean features. This fact illustrates the point that the GOAP analyst must interpret individual track information with caution to avoid errors in the analysis.

A study was also done to simulate the effect these water vapor correction errors would have on objectively contoured topographic fields. The contamination of the altimetric signals from a simulated eddy due to water vapor was substantial. When combined with the sparse data sampling and interpolation to a reference grid, eddy detection was very difficult. Water vapor data from the Special Sensor Microwave/Imager (SSM/I) in spring 1987 is sorely needed to alleviate many of the problems outlined here.

Accession For	
NTIS GRA&I	<input checked="" type="checkbox"/>
DTIC TAB	<input type="checkbox"/>
Unannounced	<input type="checkbox"/>
Justification	
By _____	
Distribution/	
Availability Codes	
Dist	Avail and/or Special
A-1	



Acknowledgments

The SEASAT Scanning Multichannel Microwave Radiometer data utilized in this technical report was processed by Frank Wentz of Remote Sensing Systems under contract N00014-83-C-0520. Discussions with M. Lybanon and J. L. Mitchell on GEOSAT matters were essential to the progress of this report. This report was supported by CNO OP-006 (formerly OP-952) under program element 63704N, Satellite Oceanography Tactical Application Program, A. E. Pressman, Program Manager.

Contents

Introduction	1
Water vapor corrections	1
Comparison of SMMR-predicted water vapor correction with cloud imagery	2
Effect of water vapor “noise” on objectively contoured mesoscale products	9
Conclusions	18
References	19

Effects of atmospheric water vapor on the detection of mesoscale oceanographic features from GEOSAT

Introduction

GEOSAT, a single-sensor satellite, carries an active microwave altimeter and was launched on 12 March 1985. The primary GEOSAT mission is to collect a global mean sea surface topography at a cross-track spacing of approximately 5 km (Mitchell, 1983). The satellite has a secondary mission of detecting and quantifying mesoscale (100–250 km) oceanographic features, such as fronts and eddies. Oceanography will become the primary objective following GEOSAT's initial 18 months in orbit when the satellite is placed in a 17-day repeat orbit for the GEOSAT Extended Repeat Mission (ERM).

The microwave altimeter relies on a measurement of pulse propagation time to determine distance from the spacecraft to the ocean surface. This time-of-travel is a function of the speed of light through the medium, which is in turn a property of the medium. Ionospheric plasma, dry atmosphere, liquid water, and water vapor are four such media encountered by the altimeter pulse on its round-trip path to the sea surface and back to the space platform.

Sea surface height corrections due to these various constituents are discussed by Tapley et al. (1982a). They calculate that variations in ionospheric electron density can cause an error of 2–20 cm in the height measurement. This effect can be modeled such that the resulting error is about 3 cm. The dry atmosphere can produce errors as large as 240 cm if left uncorrected, but fortunately these errors occur over spatial scales with wavelengths near 1000 km. Thus, media effects can be filtered out when working on mesoscale feature retrieval.

Liquid water and water vapor require an accompanying passive microwave radiometer to accurately revise the final sea surface height value. GEOSAT does not have this capability. Hence, the effect of intense rainstorms will remain in the data and produce liquid water-related errors of 10 to 100 cm. Rain will then hamper studies on such events as the doming of the sea surface (storm surge) within strong atmospheric low pressure systems, but will do little to hinder the goal of the GEOSAT Ocean Applications Program (GOAP) as described by Lybanon (1984).

The effects of vertically integrated water vapor are not as easy to overcome. The potential adjustment due to water

vapor ranges from 5 to 40 cm and can take place over the same mesoscales we wish to use in retrieving ocean fronts and eddies information. Thus, individual altimeter tracks must be screened carefully for false sea surface undulations due solely to real variations in the distribution of atmospheric water vapor. This situation might not occur if one were interested only in monthly sea surface height averages over ocean basins for use in circulation models.

A passive microwave sensor similar to the Scanning Multichannel Microwave Radiometer (SMMR) on SEASAT would provide the necessary corrections, but such a platform will not exist until the Special Sensor Microwave/Imager (SSM/I) is launched in spring 1987. This Defense Meteorological Satellite Program (DMSP) instrument will globally measure the vertically integrated water vapor to the required accuracy. However, the altimeter and radiometer would not be coincident in time, since they would be on separate platforms and some timeliness problems might arise. This report is thus directed at the effects of water vapor on retrieving ocean fronts and eddies data until the SSM/I is available to fill the void.

Water vapor corrections

The expression for the altimeter correction due to water vapor, according to Tapley et al. (1982b), is

$$\Delta h_w = \Omega \int_0^{h_e} \rho(h) dh + \eta \int_0^{h_e} \frac{\rho(h)}{T(h)} dh, \quad (1)$$

where η and Ω are constants, $\rho(h)$ is the water vapor density, h_e is the effective vapor height within the atmosphere, and $T(h)$ is the temperature profile in Kelvins. If it is assumed that a constant (adiabatic) temperature lapse rate exists and that ρ is approximately independent of altitude, Equation (1) can be integrated (Tapley et al., 1982a):

$$\Delta h_w = [0.331 - 53.3 \ln(1 - 32.5/T_o)] W, \quad (2)$$

where T_o is the temperature at the sea surface and W is the vertically integrated water vapor. A table of the coefficient in the brackets of Equation (2) versus T_o is shown in the following table:

Table 1. Water vapor correction (cm) per g/cm² at various SSTs.

[Correction cm]	T _o (C)
6.51	0
6.30	10
6.10	20
5.91	30

Table 1 reveals that the altimeter correction can change by about 10% over a 0–30°C range of SSTs. Tapley et al. (1982b) use a value of 6.36 after averaging data from several radiosondes. We use this value for the following calculations.

The area used for deriving the GOAP mesoscale product is an irregularly shaped portion of the western North Atlantic between 30–42.5°N and 50–75°W (Lybanon, 1984). In an attempt to study the potential effects of water vapor on (GOAP) altimeter data, we have restricted ourselves to SEASAT data that falls within 20–50°N and 50–80°W. Water vapor measurements from the SMMR were processed for this area, which includes the Gulf Stream system. Simultaneous visible and infrared imagery were obtained, so that besides determining the magnitude of the water vapor correction required for selected passes, we could also directly relate this error to the prevailing meteorological conditions as evidenced by cloud cover. Second, we simulate an objective altimeter data reduction algorithm to examine the effects of atmospheric water vapor variations on the final contoured topographic product.

Comparison of SMMR-predicted water vapor correction with cloud imagery

The SEASAT SMMR brightness temperatures were processed by Remote Sensing Systems using the Wentz model (1983) to retrieve the integrated atmospheric water vapor along the SMMR swath. An altimetric correction for the wet troposphere, 6.36 cm for each g/cm² of vertically integrated water vapor, was applied to the SMMR passes (Tapley et al., 1982b). These data were then scanned for examples of rapid spatial gradients in the altimeter correction, which might give rise to false alarms in the detection of oceanic eddies. This worst-case series of altimetric corrections was then compared with infrared images of cloud patterns from the Geostationary Operational Environmental Satellites-East (GOES-E). The purpose was to

identify the weather patterns responsible for anomalously large corrections to the altimeter signal in the Gulf Stream region.

Three examples are presented in Table 2; dates and times of the passes are included.

Table 2. SEASAT orbits used for water vapor versus cloud imagery comparisons.

Figure #	Rev #	Date	Time (SEASAT)	Time (GOES)
1	320	19 Jul 78	0925Z	0930Z
2	945	1 Sep 78	0215Z	0930Z
3	952	1 Sep 78	1325Z	1600Z

Two sets of imagery are presented here to understand the relationship between the water vapor sensed by the SMMR and the associated meteorological events. Figures 1a, 2a, and 3a are GOES-E infrared images that cover the western North Atlantic from Cuba to Nova Scotia and the U.S. east coast to approximately 57°W. This large synoptic scale view allows one to easily grasp the weather patterns present at the times of the SEASAT overpasses. Figures 1b, 2b, and 3b are higher resolution subsections of the (a) images and provide the close-up view required to adequately resolve the mesoscale atmospheric events.

On 19 July 1978 (Fig. 1a), an old cool front was positioned near the North Carolina coast. A weak low-pressure system was forming along this front off Cape Hatteras and a second cool front trailed toward the southwest down into the Bahama Islands. Warm, moist tropical air was positioned below the northernmost front, which stretched along 38°N with cooler, drier air to the north near Cape Cod. In general, a decrease in water vapor content would be anticipated as the satellite ascended from the southeast through the cool front into the cool shelf waters.

The high-resolution subsection (Fig. 1b) also includes an overlay with the ascending SEASAT SMMR water vapor correction values (cm) plotted along the track with tick marks every 110 km. The data clearly indicates a rise in water vapor correction as SEASAT approached the southern fringe of the cool front, and then the correction trails off to a value of about 10 cm just north of the front. This drop of 13–15 cm occurs over a distance of 250 km. This case has several points of interest: the maximum water vapor value is located on the southern boundary of the cloud features; each cloud feature has its own spike in the water vapor curve; and both occur over the Gulf Stream system, where numerous mesoscale ocean features have sea surface height signatures ranging from 20 to 100 cm.

From 1 September to 4 September 1978, Hurricane Ella followed a track northwestward over the North Atlantic

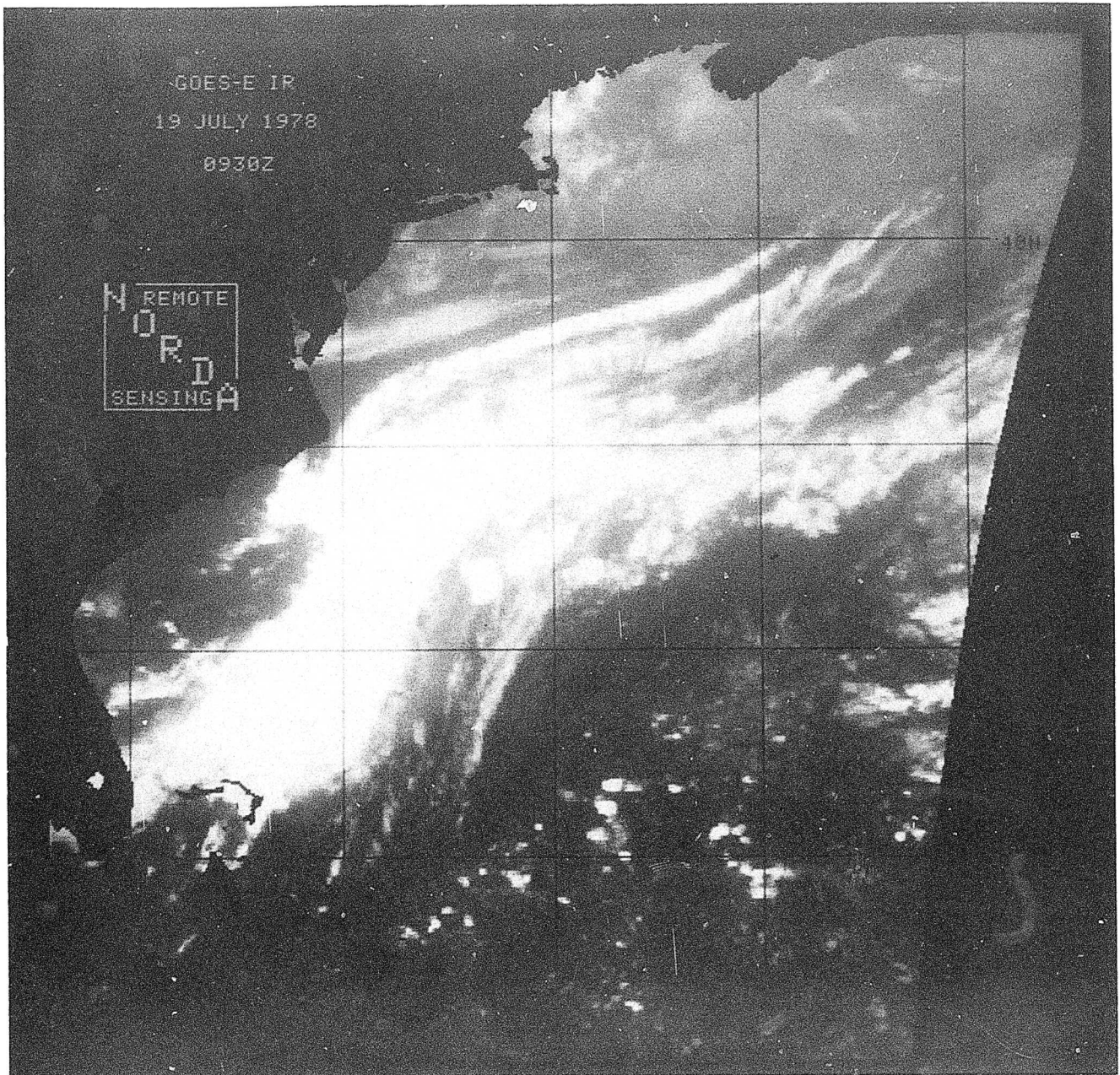


Figure 1a. Infrared (IR) image from GOES-E on 19 July 1978, 0930Z covering the GEOSAT demonstration region, with 5° latitude-longitude grid.

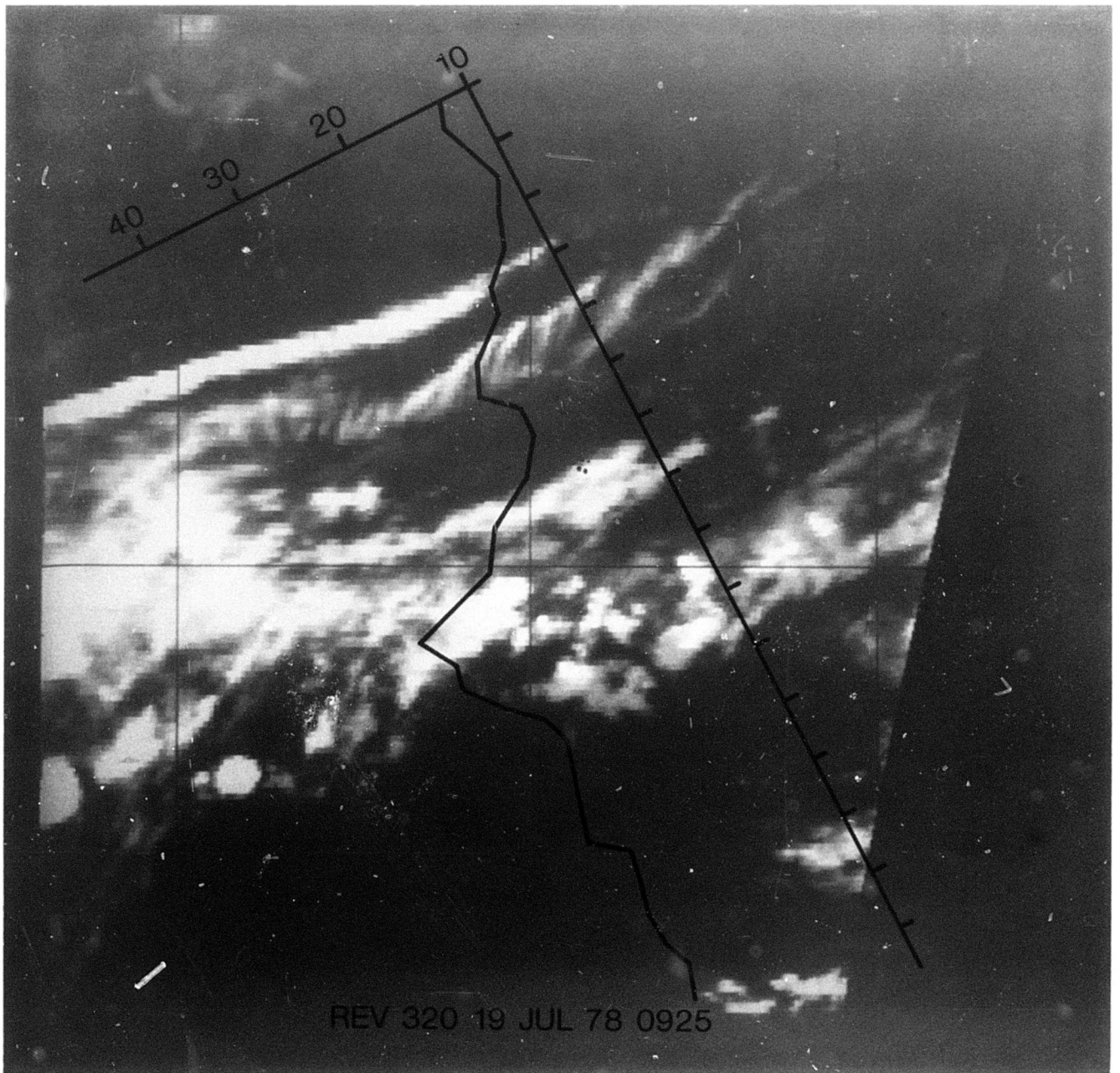


Figure 1b. High-resolution subsection of Figure 1a (without land mask) including overlay of SEASAT SMMR water vapor corrections (cm) along middle of SMMR swath. Tick marks located every 110 km.

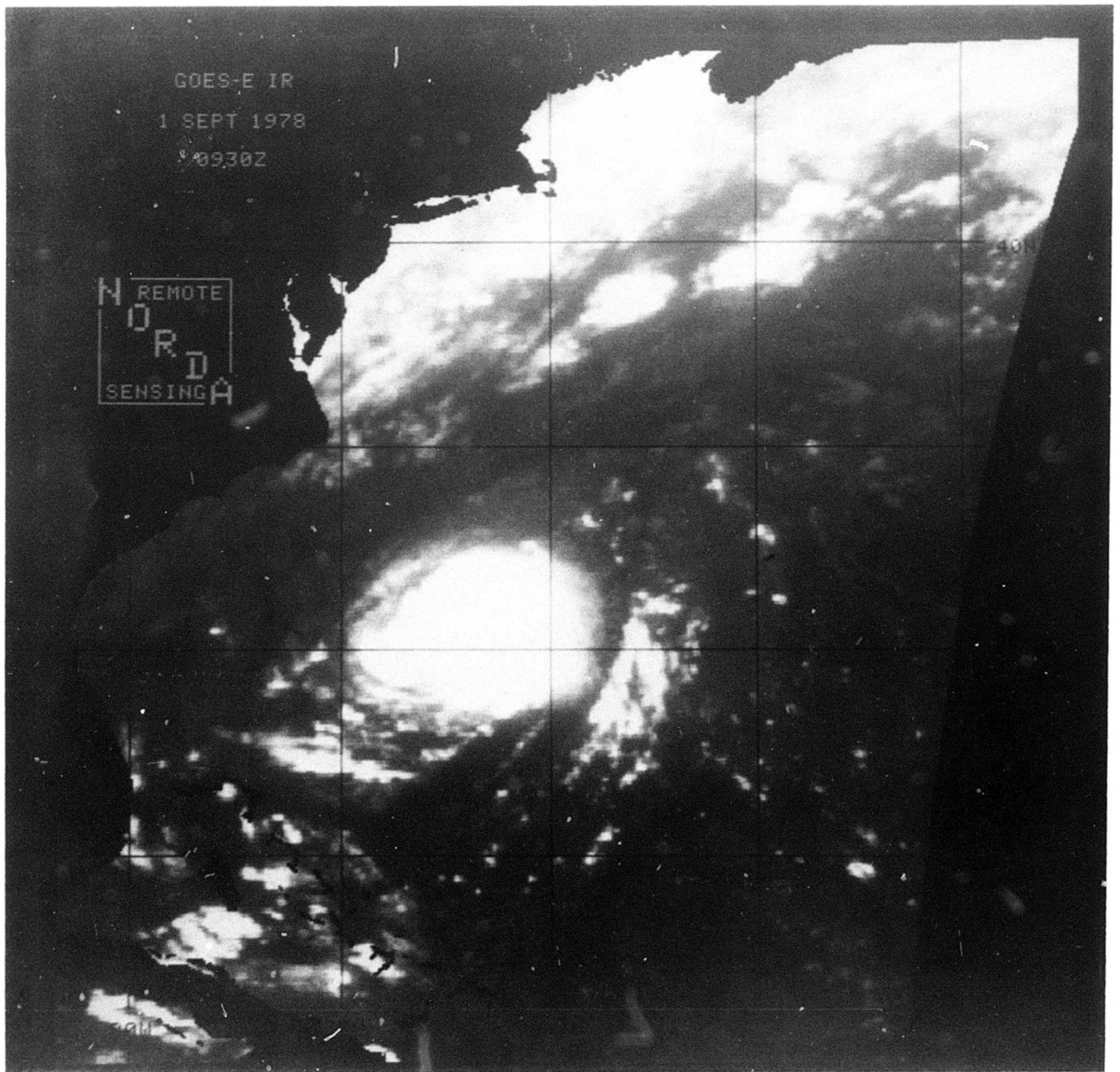
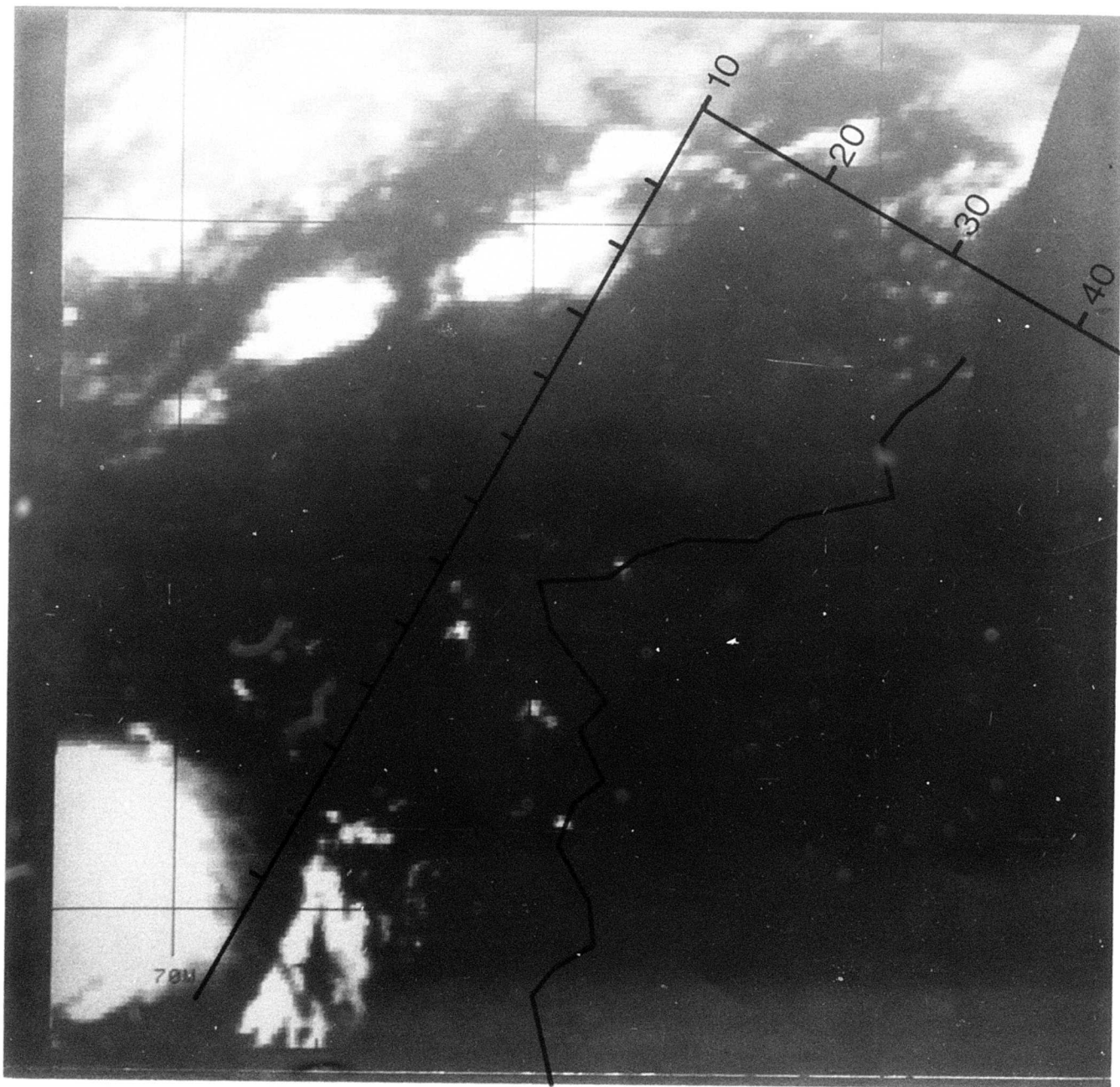


Figure 2a. Infrared (IR) image from GOES-E on 1 September 1978, 0930Z.



REV 945 1 SEP 78 0215

Figure 2b. High-resolution subsection of Figure 2a including overlay of SEASAT SMMR water vapor corrections (cm).

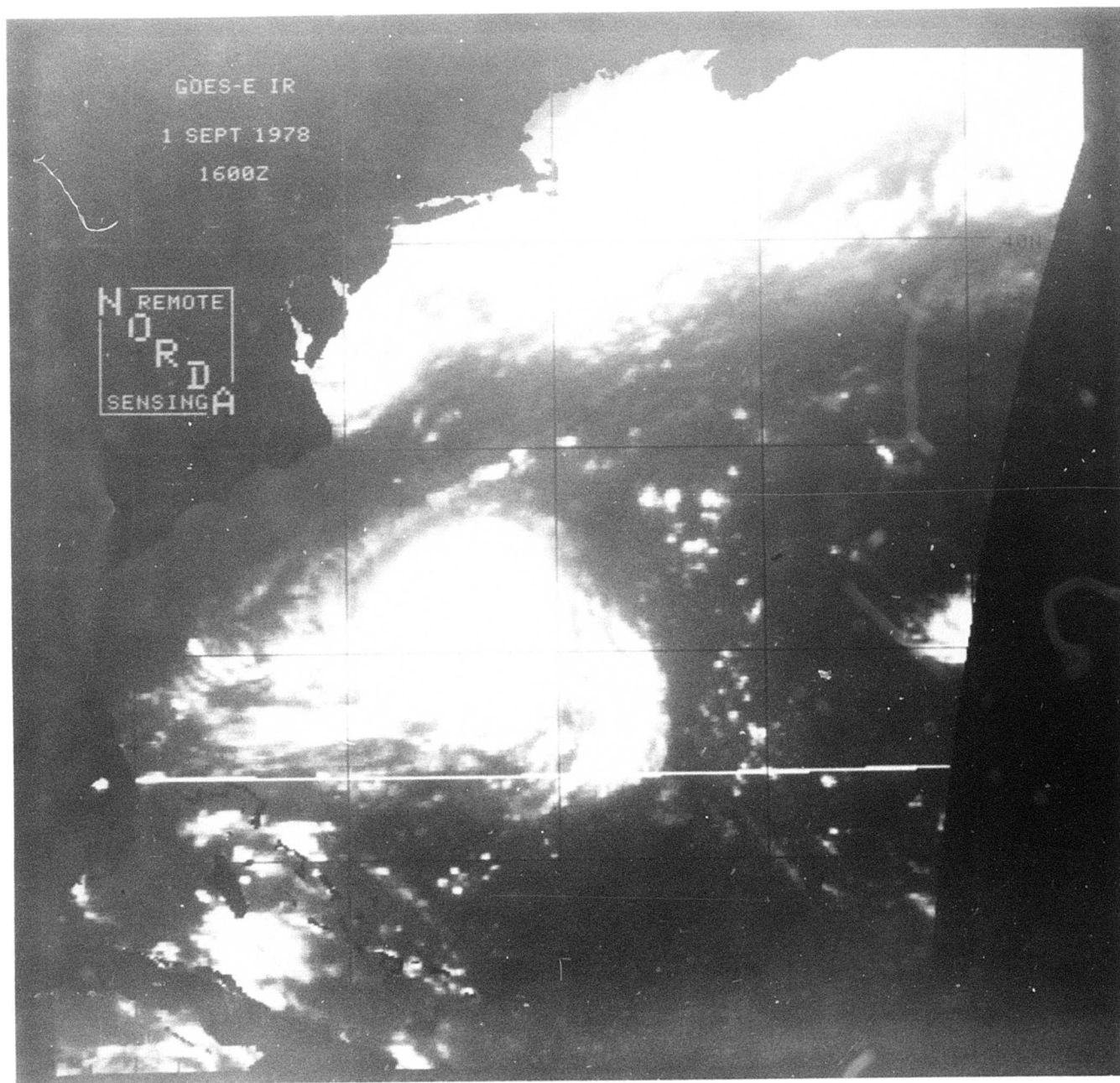
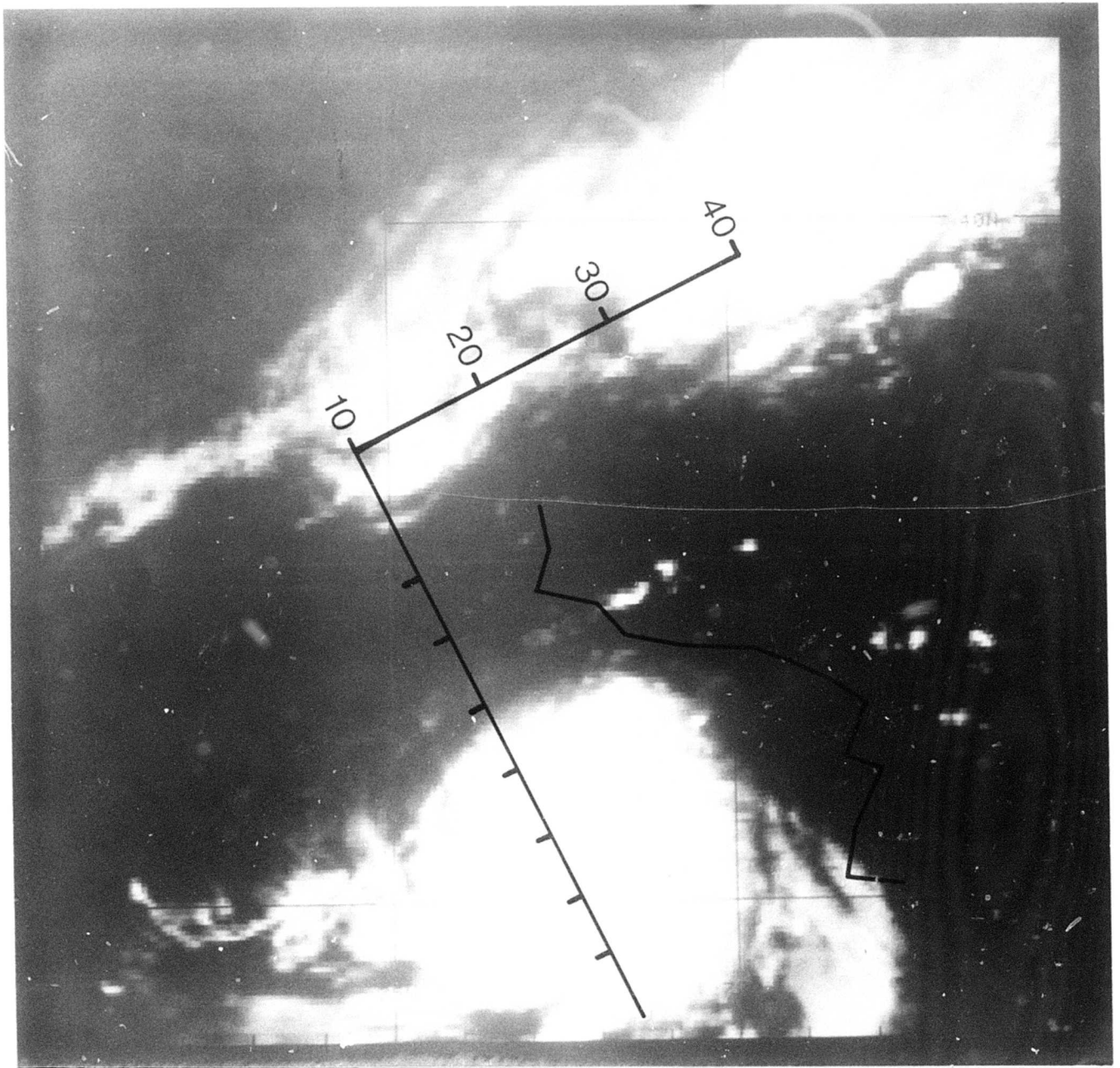


Figure 3a. Infrared (IR) image from GOES-E on 1 September 1978, 1600Z.



REV 952 1 SEP 78 1600

Figure 3b. High-resolution subsection of Figure 3a including overlay of SEASAT SMMR water vapor corrections (cm).

to about 31°N, 73°W where it abruptly changed course to the northeast in response to an advancing upper level trough of low pressure (Hawkins and Black, 1983). The small, compact nature of this 110-mph hurricane is displayed (in Fig. 2a) shortly before it stalled and turned northeastward. Note the general lack of clouds in the periphery of the storm and the cold frontal band of clouds to the north.

Figure 2b combines the high-resolution imagery with the descending orbit's water vapor corrections. The track extends from the moist southern end of the cold front southwestward to the vicinity of the hurricane. Two sharp water vapor boundaries are associated with this particular set of meteorological conditions. The minimum occurs in an area of few clouds between the storm and the cold front caused by subsidence of warm, dry air aloft associated with the large, strong anticyclone above the hurricane. The strength of this phenomenon, as measured by the SMMR and shown here in terms of water vapor correction, indicates that the storm is well entrenched and is pumping huge quantities of air up through the low level cyclone and then out and down the periphery of the storm.

Very sharp gradients of 10 cm or so occur over spatial scales of approximately 110 km, while changes of 20 cm are evident over distances of 200–250 km. Note that these water-vapor-induced fluctuations take place well south of the cold frontal boundary where one would expect some homogeneity in the tropical air mass in the absence of a hurricane. The hurricane has thus modified the entire atmospheric moisture profile over this Gulf Stream region such that false gradients in the sea surface heights would be inferred if the moisture were not appropriately taken into account. It should be noted that it is highly unlikely that the GOAP analyst will not be aware of this meteorological phenomenon when using it for individual track information, but if many passes are combined into an ensemble average, this spike in the data could be misleading.

Figure 3a (1 September 1978, 1600Z) pictures the storm at roughly its westernmost position before turning northeastward. The distance between the hurricane and the cold front has clearly decreased in the 6½ hours since Figure 2a. Thus, one might expect the water vapor gradients to increase in magnitude, which indeed is the case, as illustrated in Figure 3b. Ascending rev 952 cuts across the storm and proceeds northwestward into the zone of dry air caused by the subsidence. The resulting atmospheric correction would have been 22 cm over a distance of 180 km and in a direction that would reduce the normal Gulf Stream altimetric signature.

Several examples of large water vapor corrections without accompanying GOES-E imagery are exhibited in

Figures 4 and 5. All cases reveal 15-cm changes occurring within distances less than 200 km, with some considerably sharper. This type of false signal would not mask the sharp characteristics of the north wall of the Gulf Stream or relatively new warm- or cold-core rings, but it could cause considerable difficulty when trying to detect old cold-core rings. These cold rings often rapidly lose their surface thermal signature and a significant portion of their original dynamic height profile. An altimeter used for detecting these small, but important, ocean features must be corrected for water vapor or the ring must be observed under a relatively homogeneous moisture field. Otherwise, one of the altimeter's strong points over infrared imagery will be rendered useless.

In summary, altimeter passes over the North Atlantic can encounter moisture fronts representing the separation of warm, moist air masses to the south and cooler, dryer air to the north as well as other phenomena. The summer lifetime of SEASAT gave us a unique view of the atmospheric moisture gradients associated with hurricane environmental conditions. Instead of exhibiting a sharp water vapor gradient associated with the core of the storm (missing due to a lack of resolution), the data identified a peripheral area of strong subsidence where descending air has dried extensively and thus created a water vapor discontinuity.

However, none of the meteorological conditions sampled by SEASAT in the GOAP area are worst-case situations. Cold fronts in fall and spring can cause extremely sharp boundaries to exist over very small distances. Water vapor corrections of 30 cm are possible on spatial scales of less than 100–200 km. If left uncorrected, these error sources can make individual altimeter tracks very difficult to interpret.

Effect of water vapor "noise" on objectively contoured mesoscale products

GOAP would benefit from the automation of as many analysis and dissemination functions as possible. In particular, the process of resolving mesoscale features from the altimeter time series can, to some extent, be automated through smoothing and objective data contouring (Mitchell, 1983). The end result would be as objective a topography map as possible. This section addresses the problems induced by not making water vapor corrections while still trying to objectively contour the data fields.

One such contouring procedure was developed at the Kansas Geological Survey as part of a library of functions called "Surface-II Graphics System" (Sampson, 1978). The

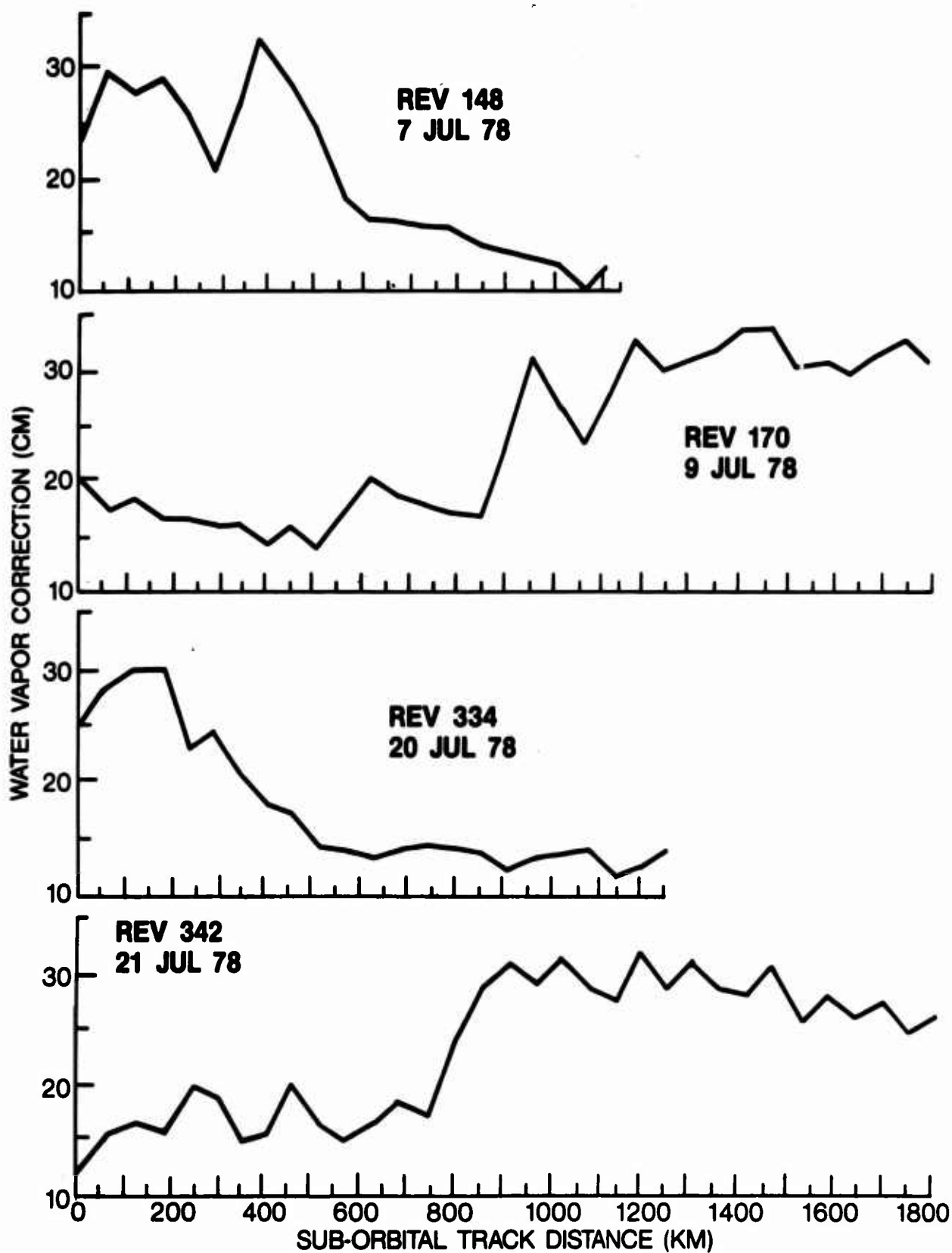


Figure 4. Examples of SEASAT data revealing large water vapor correction gradients over short mesoscale distances.

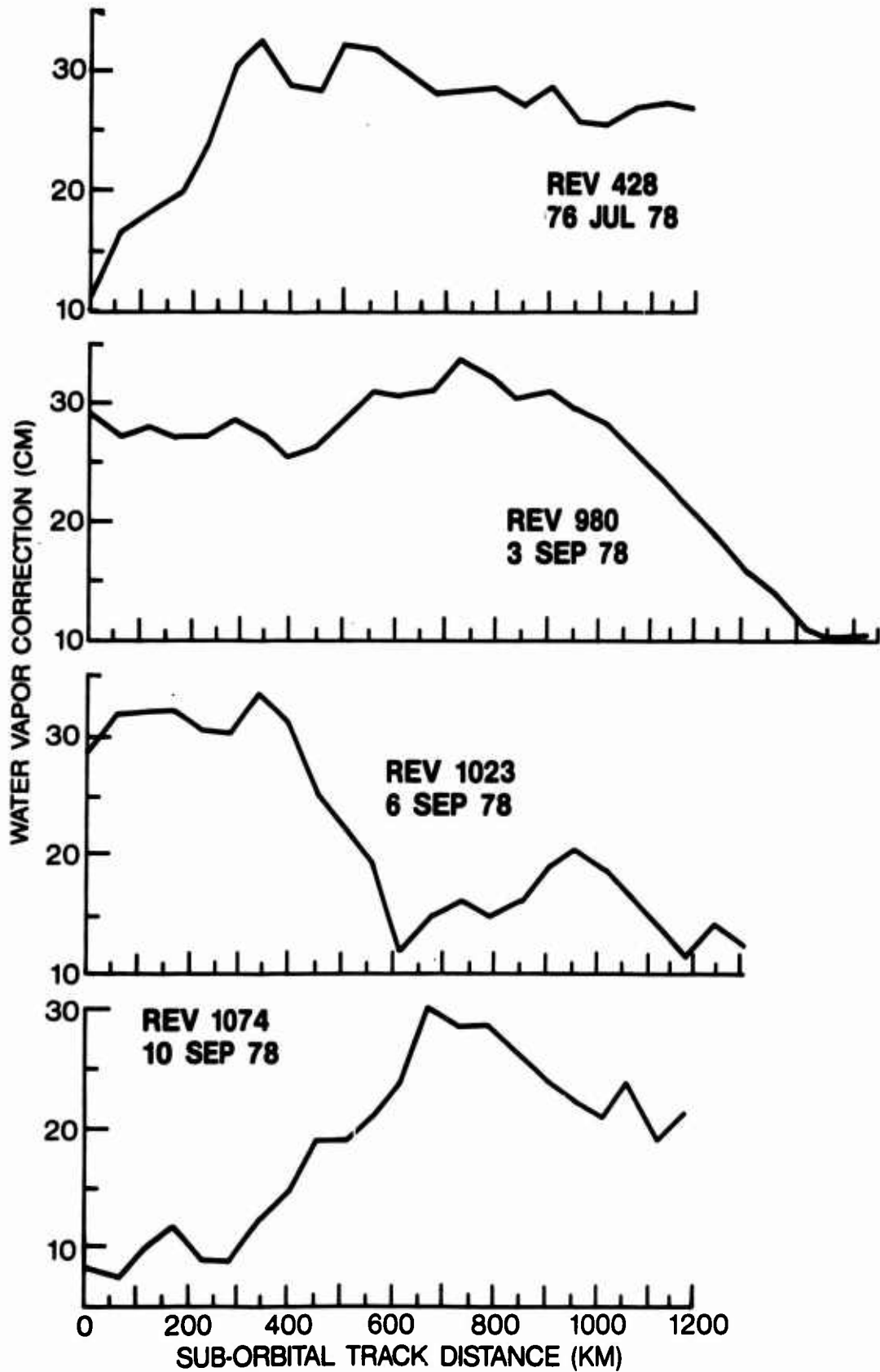


Figure 5. Examples of SEASAT data revealing large water vapor correction gradients over short mesoscale distances.

procedure involves interpolating the altimeter data to a rectangular grid and subsequently contouring the gridded data. The interpolation is accomplished by summing the contributions from each altimeter data point divided by the distance-squared to the observation point. This scheme does a good job of representing a topographic "hill" as long as the highest point is located between two altimeter passes.

Any time-dependent signals superimposed on the altimeter data will be interpreted as spatial variance in the structure of the mesoscale contours, since this method incorporates data from satellite passes that occurred intermittently over a given period. To assess the effect of spatial variability in atmospheric moisture, we introduced SEASAT moisture data into a simulated GEOSAT altimeter data stream. The process is described as follows:

- Model the eddy as a Gaussian function of x and y with a 50-km standard deviation and a diameter of 200 km.
- Construct altimeter data sets that would result from a given set of orbital elements over a prescribed interval of time. Allow for the advection of the eddy when appropriate.

- Add to these altimeter data sets corrections due to moisture as measured by the SEASAT SMMR for similar passes at the same latitude.
- Interpolate this data to a rectangular grid 41 x 41 according to the prescription:

$$h_{ij} = \frac{\sum_{k,l} H_{k,l} / r_{ijk}^2}{\sum_{k,l} 1 / r_{ijk}^2}$$

where k refers to the k th orbit; and l designates a height measurement, H ; and i and j refer to an observation grid point (Sampson, 1978). The interpolated value of the sea surface height is h and r is the distance from the (k, l) th observation point to the (i, j) th grid point.

- Contour the grid at 10-cm intervals and 5 cm when necessary.

The surface profile of the model eddy used in this study is shown in Figure 6. Maximum height was set at 70 cm with a 2σ (standard deviation) set at a 100 km diameter while the eddy was given an outer dimension of 200 km

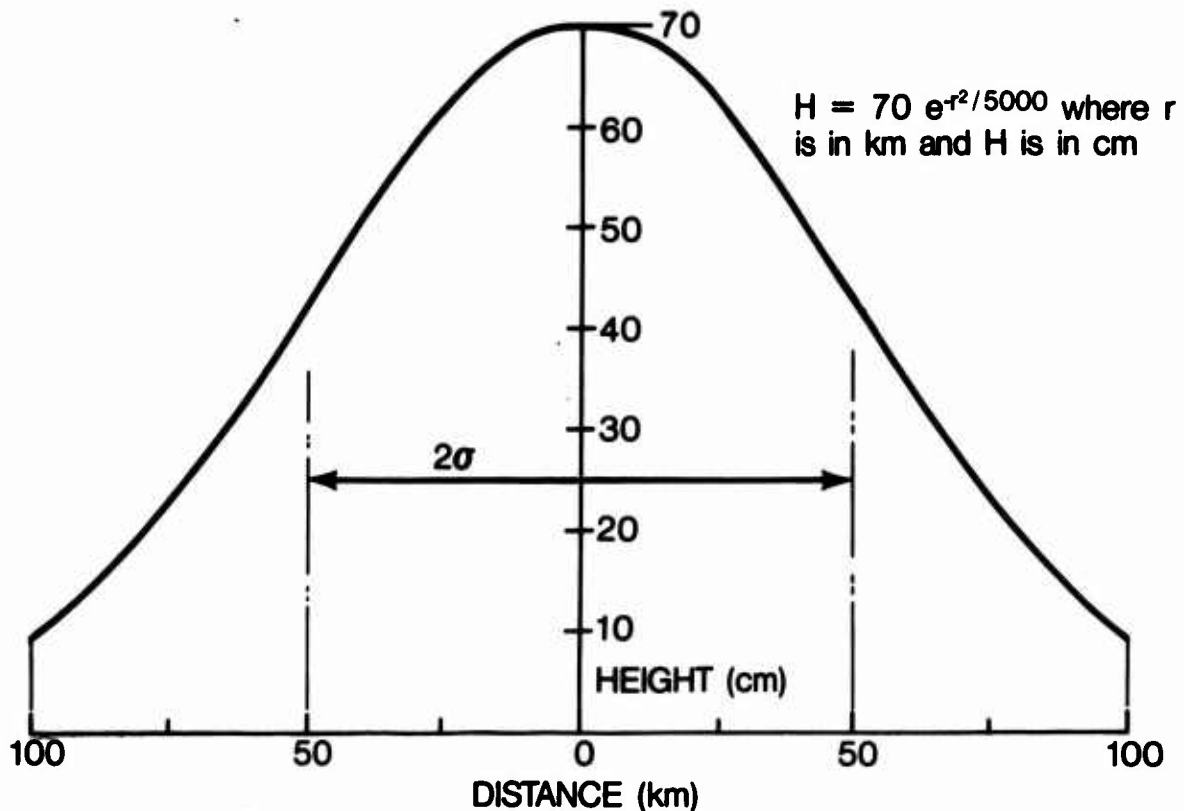


Figure 6. Graphic representation of model eddy used in sampling experiment.

for its diameter. For the first trial, the planned prelaunch GEOSAT orbit is used and integrated over a time interval of 12 days. A sampling of orbital ground tracks is shown in Figure 7a, where each orbit is labeled by its rev number. The pattern shows four ascending and four descending tracks, each separated from the other by approximately 40 km. We then position the eddy in the center of the diamond and allow it to be advected at a constant velocity of 4 km/day toward the west. The model eddy is sampled each time the altimeter passes over, and the grid is formed after 12 days of data are collected. The grid is then contoured.

Figure 7a illustrates the spatial scales involved by overlaying the satellite tracks on the model eddy. Eddy position for day 1 and day 12 are shown via the two solid and two dashed contours. The inner circle ($r = 50$ km) represents the 1σ of our model eddy (i.e., the Gaussian shape of the eddy sea surface height profile was specified such that $1\sigma = 50$ km as seen in Figure 6). The second or outer circle depicts the cutoff radius of 100 km (diameter = 200 km). These values were selected to approximate real Gulf Stream eddies, realizing that they come in a wide variety of shapes and sizes. The eddy location on day 12 represents a westward drift of 4 km/day (about 50 km net displacement during the course of the experiment).

These prelaunch GEOSAT tracks lay down 40 km apart every 3 days (approximately every 43 orbits). Figure 7b is an objectively contoured plot of the eddy sea height field using data points sampled during each of the four passes over the model eddy using a 10-km grid. The eddy in Figure 7b is stationary and is centered within the crossover of four ascending and four descending orbits. The eddy mapping accomplished with these simulated satellite passes represents a plausible representation of the original eddy. The peak height of 70 cm has decreased to less than 50 cm, but the general shape and magnitude is reasonable.

Figure 7c reveals that eddy advection to the west (4 km/day) moves the resampled eddy to the western portion of the altimeter crossovers and reduces the maximum sea surface height from 70 cm to less than 50 cm. Thus, this warm core eddy has lost about 30% of its magnitude. Note that its size has also decreased, but the eddy would likely still be readily detected using this methodology. Note that remapping to a 10-km grid also promotes some loss of eddy intensity.

Figure 7d includes the effects of water vapor attenuation as measured in the actual SEASAT orbits annotated within Figure 7a. The water vapor in the atmosphere slows down the altimeter pulse and increases the round trip travel

time, which has the effect of lowering sea surface topography measurements if no correction is made. Therefore, when each pass in Figure 7d is contaminated by water vapor distributions observed in this same location during SEASAT overflights, and when the eddy's motion is included, the resulting contour map is quite fragmented.

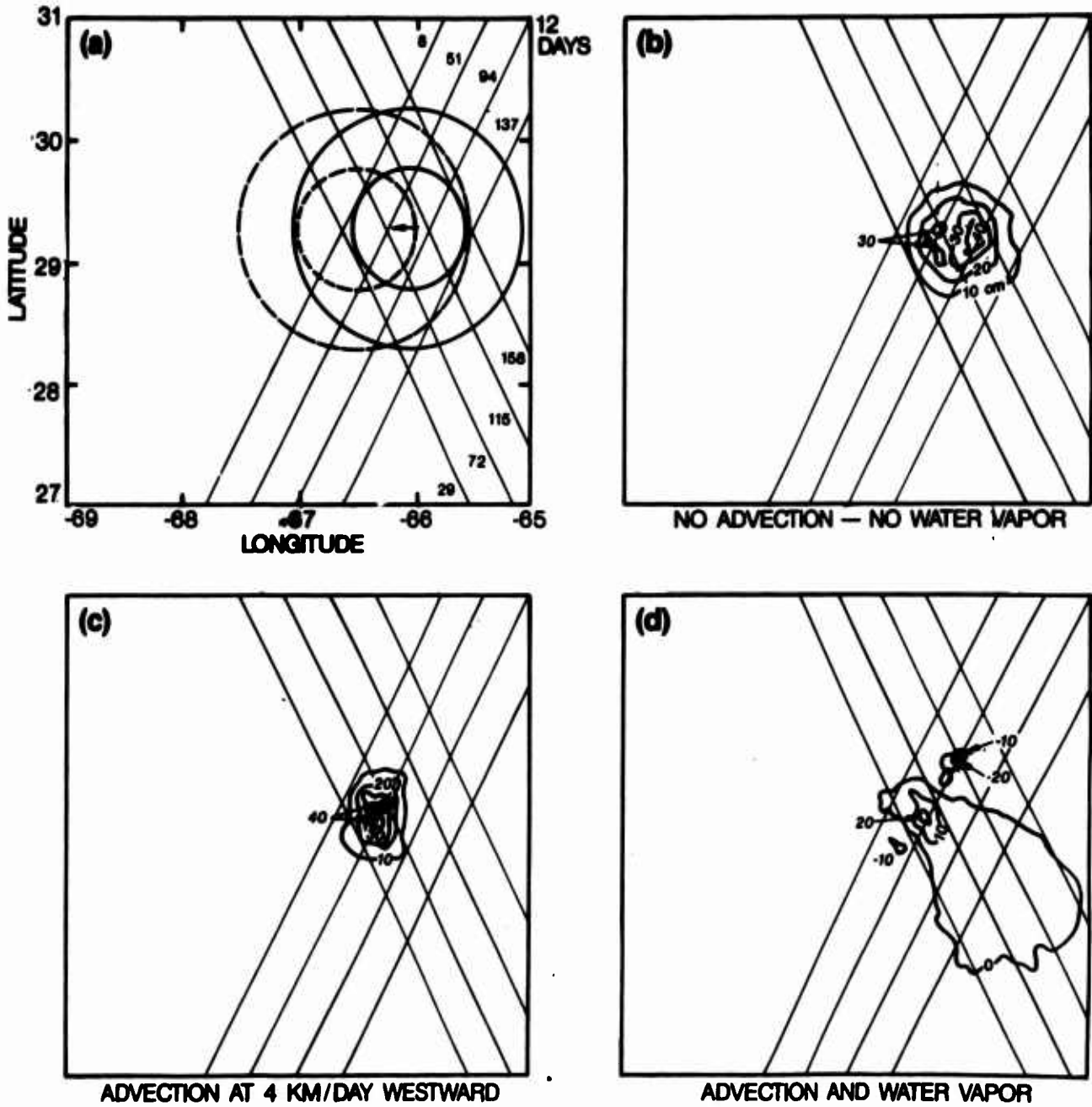
Figure 7d clearly illustrates the impact that water-vapor-induced phase delays can have on detecting ocean mesoscale features using uncorrected altimeter measurements. The model eddy is no longer a prominent identifiable water mass, but is now smeared beyond recognition. The distortion would be more severe if we had added realistic topographic noise around the eddy. Thus, the magnitude and spatial scales associated with atmospheric water vapor contamination can readily mask the sea surface signatures of Gulf Stream warm core eddies.

Our first case was an optimistic version where the eddy was in the best possible viewing location. Case II (Figs. 8a-d) depicts the objective mapping of our model eddy when it is initially positioned south of the optimum crossover position. Figures 8b, c resemble their counterparts in Figure 7b, c with only minor changes in shape, due mainly to sparse data sampling. Note again how the effects of water vapor delay degrade the eddy to a point where it would not be detectable.

GEOSAT did not reach its planned prelaunch orbit, but was injected into a more elliptical orbit with a slightly different period. The resulting track laydown sequence provides for an initial track separation of 80 km at 40°N after 3 days and another track located 40 km from the original one after 26 days. This orbit differs from the planned GEOSAT orbit in that, locally, an adjacent track separation of 40 km will not be achieved until 26 days versus the previously planned 3 days.

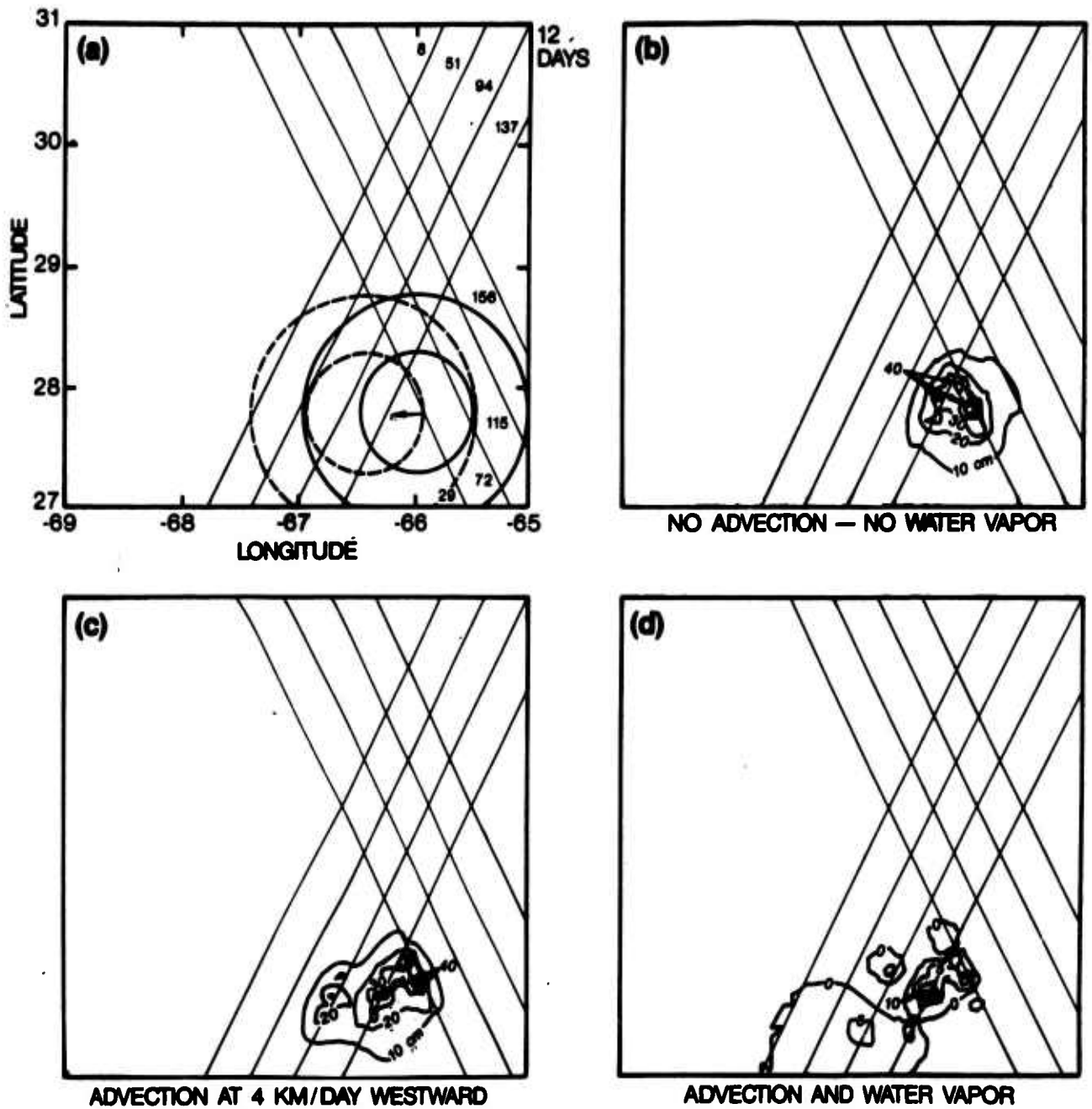
To examine the consequences of the actual GEOSAT orbit used during its first 18-month geodetic mission, we present Case III where a 26-day integration time is applied to the altimeter data for our simulated eddy. Figure 9a exhibits the model eddy with real GEOSAT ground tracks 80 km apart after 26 days. One can readily see the effect of such sparse sampling with just four tracks. This is borne out in the subsequent plots, especially Figure 9c, where an apparent double-peaked eddy is retrieved. Figure 9d again reveals that water vapor contamination obscures the eddy's topographic signal in combination with poor sampling.

Finally, we assess what information might be extracted near the cross-over point of ascending and descending passes separated in time by about 3 days using the actual GEOSAT orbit (Fig. 10a). Our model eddy can be detected



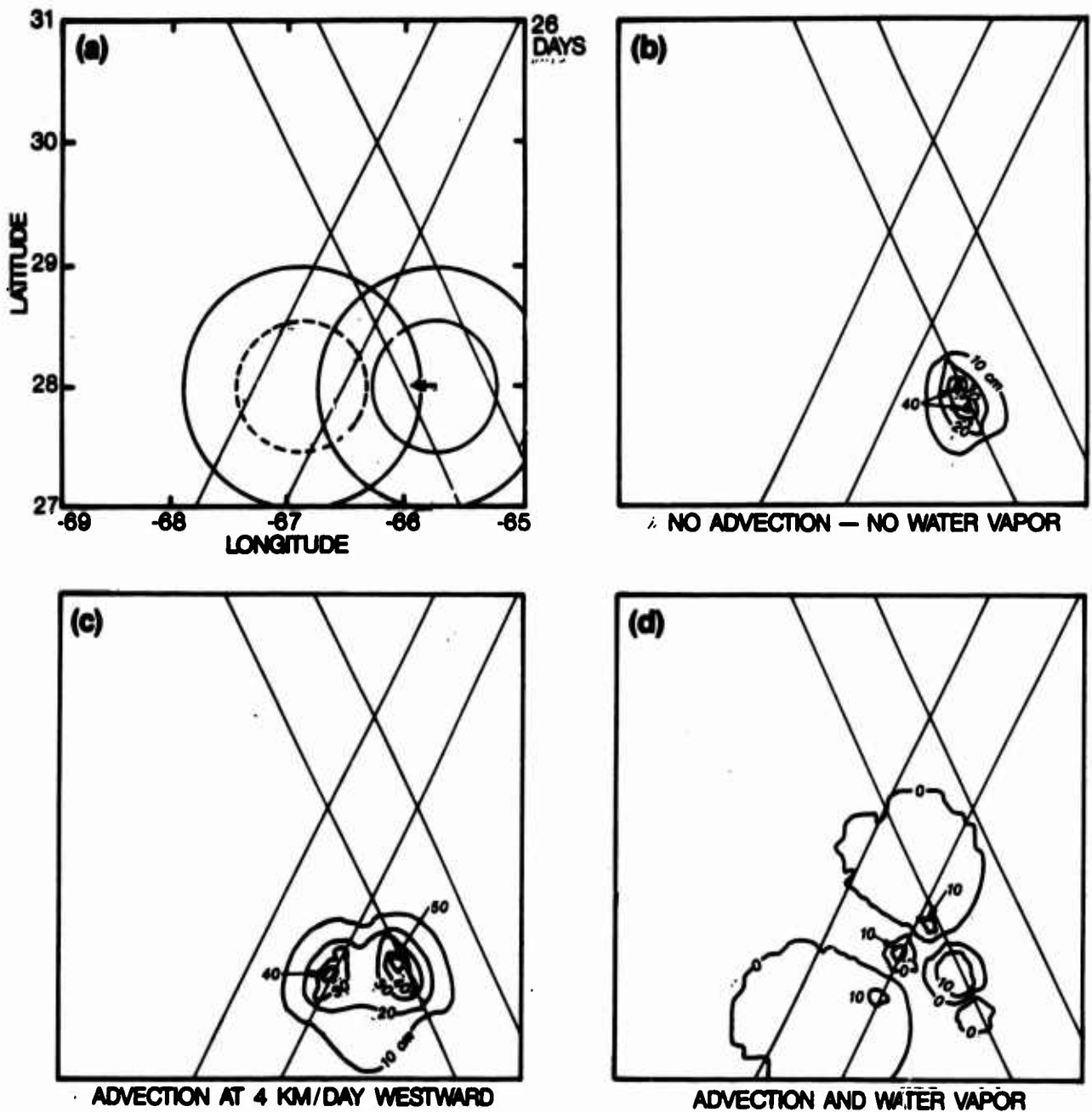
Case I

Figure 7. (a) Coverage of prelaunch GEOSAT altimeter tracks over the model eddy, (b) sea surface height contours interpolated to grid for eddy with no motion, (c) with 4 km/day movement to the west, and (d) with additional impact of adding water vapor errors into data.



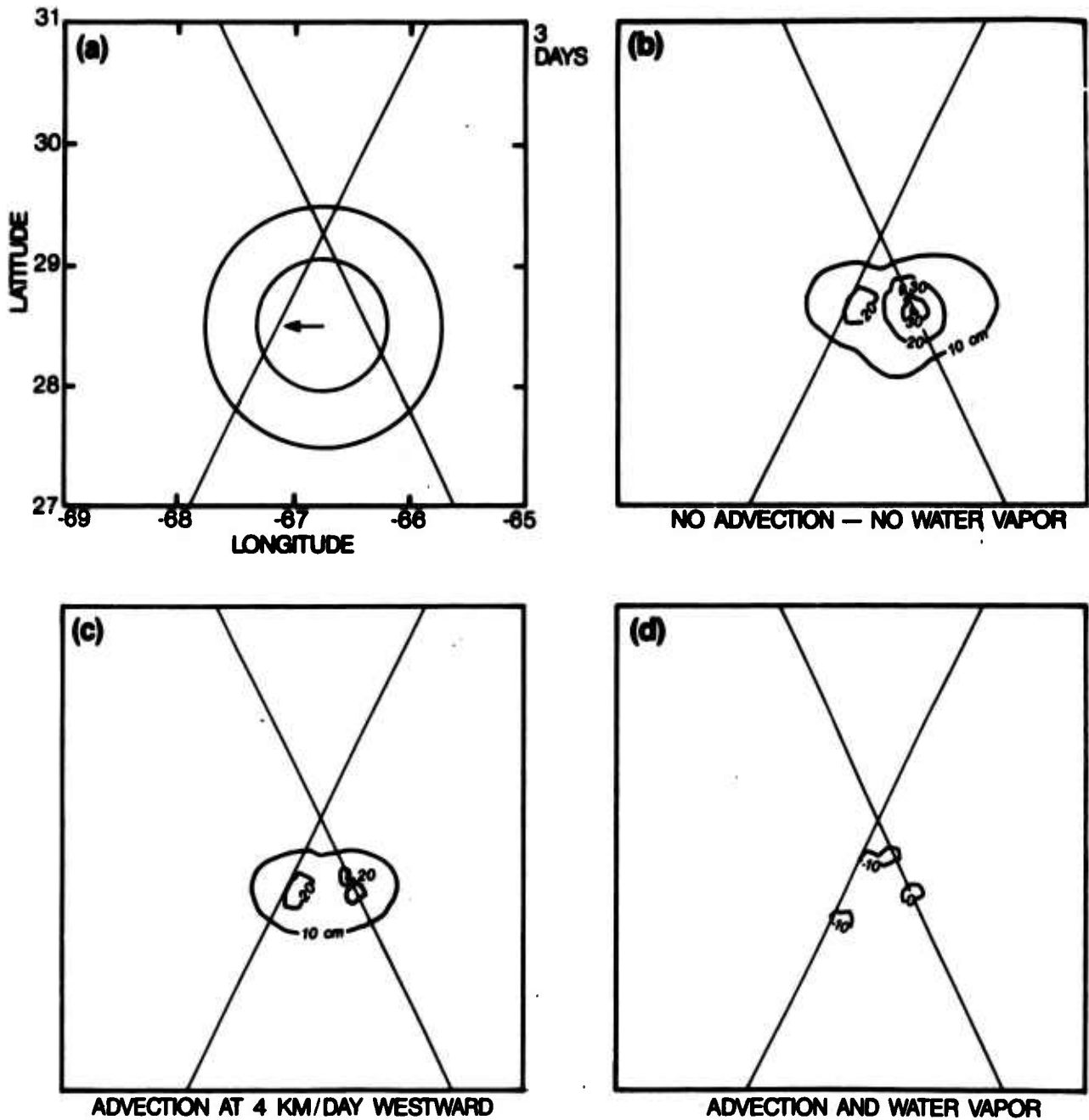
Case II

Figure 8. Same as for Figure 7, except with model eddy now located below the area of best data sampling.



Case III

Figure 9. (a) Coverage of actual GEOSAT altimeter after 26 days over same model eddy, (b) height contours with stationary eddy, and (c) addition of advection and water vapor errors.



Case IV

Figure 10. (a) Coverage of actual GEOSAT altimeter after 3 days over model eddy in Gulf Stream, (b) height contours with stationary eddy, and (c) additional effect of movement and water vapor errors.

when no advection or water vapor is added (Fig. 10b), but its intensity has decreased by a factor of two. The inclusion of advection distorts the topographic contours (Fig. 10c) while water vapor attenuation and advection (Fig. 10d) totally mask out the model eddy's signature.

The eddy sampling simulations presented in our four case studies readily reveal the damaging impact uncorrected water vapor delays can cause when trying to map mesoscale fronts and eddies. The SEASAT SMMR water vapor values used here clearly show that discontinuities in the water vapor field do occur on the same spatial scales of the eddy field. It should be noted that this data set (Case I-IV) does not represent the worst case, since these were all summertime orbits and do not include the effects of tropical cyclones. Wintertime Gulf Stream conditions would contain numerous examples with sharper water vapor gradients associated with strong cold fronts.

Therefore, the use of a limited number of altimeter passes to objectively map the front and eddy field will be significantly hindered by variations in the water vapor field. The GOAP effort in eddy identification and analysis has succeeded because the human analyst is able to combine the best that IR and altimeter data have to offer. Objective mapping without water vapor corrections will be difficult, if not impossible, to interpret as illustrated in this report.

The GEOSAT Extended Repeat Mission, similar to the SEASAT 3-day repeat cycle, will provide better sampling as far as mapping fronts and eddies is concerned. The successful launch of the SSM/I in spring 1987 should produce water vapor corrections that will significantly negate the problems outlined in this report.

Conclusions

The SMMR data obtained from SEASAT demonstrates that height corrections due to atmospheric moisture can reach 20-40% of the eddy signature over spatial scales that match those of oceanic eddies. Hence, the moisture can either mask or distort an existing eddy or produce a false alarm where no eddy exists. By analyzing cloud patterns from satellite data, the analyst may be able to reach a qualitative conclusion as to the accuracy of a given altimeter time series. When the SSM/I is launched, adequate global atmospheric data (albeit not boresighted) will

exist with which to quantitatively correct the altimeter for water-vapor-induced errors.

It is unfortunate that SEASAT did not have the opportunity to operate during the Northern Hemisphere winter. Strong Arctic cold fronts moving out over the east coast of the U.S. would have produced much stronger water vapor gradients on the mesoscale spatial scale. Atmospheric water vapor corrections of 25-30 cm in the Gulf Stream area likely occur and will present an additional problem to the GOAP analyst. This paper does not attempt to identify similar conditions in the Southern Hemisphere (SEASAT winter), since we are restricting research to the GOAP Gulf Stream region.

The SEASAT passes near Hurricane Ella reveal that large atmospheric water vapor corrections are required as the sensor data transitions from the warm, dry air in the outlying subsidence area to the moist, central rain band region of the front to the north or the hurricane to the south. The maturity of the storm is thus reflected in the strength of the subsidence band related to the upper level anticyclone. The magnitude of the correction over mesoscale spatial scales ranges from 10 to 20 cm. This gradient was not expected to approach the magnitude found here.

Objective mapping via our simulated altimeter flights over a warm core ring (sea surface height = 70 cm) clearly demonstrates the problems associated with water vapor contamination. The water-vapor-induced delay of the altimeter pulse causes the sea surface topographic signature of the eddy to drop markedly so as to become obscured by the noise field. When combined with advection of the eddy through the grid and problems with remapping, even on a 10-km grid, detection of the simulated eddy did not always occur. Caution must therefore be taken when attempting to objectively contour altimeter sea heights that have not been corrected for water vapor attenuation.

It should be noted that a 70-cm topographic signal represents a relatively strong eddy. Many of the Gulf Stream rings one wishes to detect have values closer to 50 cm, and some older rings are characterized by 25 cm sea height differentials. These rings would be impossible to locate using data that is uncorrected for water vapor via an objective mapping routine. However, on the other hand, the north wall of the Gulf Stream and its 120-150 cm rise would be easily detected by a number of techniques.

References

Hawkins, J. D. and P. G. Black (1983). SEASAT Scatterometer Detection of Gale Force Winds Near Tropical Cyclones. *Journal of Geophysical Research*, v. 88, pp. 1674-1682.

Lybanon, M. (1984). *GEOSAT Ocean Applications Program (GOAP) Initial Data Processing and Analysis System Test and Evaluation Plan*. Naval Ocean Research and Development Activity, NSTL, Mississippi, NORDA Technical Note 270, 29 pp.

Mitchell, J. L. (1983). *A Position Paper: Mesoscale Oceanography From GEOSAT*. Naval Ocean Research and Development Activity, NSTL, Mississippi, NORDA Technical Note 226, 25 pp.

Sampson, R. J. (1975). *Surface II Graphics System* (Revision 1). Kansas Geological Survey, Lawrence, Kansas.

Tapley, B. D., G. H. Born, and M. E. Parke (1982a). The SEASAT Altimeter Data and its Accuracy Assessment. *Journal of Geophysical Research*, v. 87, pp. 3179-3188.

Tapley, B. D., J. B. Lundberg, and G. H. Born (1982b). The SEASAT Altimeter Wet Tropospheric Range Correction. *Journal of Geophysical Research*, v. 87, pp. 3213-3220.

Wentz, F. J. (1983). A Model Function for Ocean Microwave Brightness Temperatures. *Journal of Geophysical Research*, v. 88, pp. 1892-1908.

ADA176365

REPORT DOCUMENTATION PAGE					
1a. REPORT SECURITY CLASSIFICATION Unclassified		1b. RESTRICTIVE MARKINGS None			
2a. SECURITY CLASSIFICATION AUTHORITY		3. DISTRIBUTION/AVAILABILITY OF REPORT Approved for public release; distribution is unlimited.			
2b. DECLASSIFICATION/DOWNGRADING SCHEDULE					
4. PERFORMING ORGANIZATION REPORT NUMBER(S) NORDA Report 126		5. MONITORING ORGANIZATION REPORT NUMBER(S) NORDA Report 126			
6. NAME OF PERFORMING ORGANIZATION Naval Ocean Research and Development Activity		7a. NAME OF MONITORING ORGANIZATION Naval Ocean Research and Development Activity			
6c. ADDRESS (City, State, and ZIP Code) Ocean Science Directorate NSTL, Mississippi 39529-5004		7b. ADDRESS (City, State, and ZIP Code) Ocean Science Directorate NSTL, Mississippi 39529-5004			
8a. NAME OF FUNDING/SPONSORING ORGANIZATION Naval Ocean Research and Development Activity	8b. OFFICE SYMBOL <i>(If applicable)</i>	9. PROCUREMENT INSTRUMENT IDENTIFICATION NUMBER			
8c. ADDRESS (City, State, and ZIP Code) Ocean Science Directorate NSTL, Mississippi 39529-5004		10. SOURCE OF FUNDING NOS.			
		PROGRAM ELEMENT NO. 63704N	PROJECT NO.	TASK NO.	WORK UNIT NO.
11. TITLE (Include Security Classification) Effects of Atmospheric Water Vapor on the Detection of Mesoscale Oceanographic Features from GEOSAT					
12. PERSONAL AUTHOR(S) Jeffrey D. Hawkins and Peter M. Smith					
13a. TYPE OF REPORT Final	13b. TIME COVERED From _____ To _____	14. DATE OF REPORT (Yr., Mo., Day) November 1986	15. PAGE COUNT 21		
16. SUPPLEMENTARY NOTATION					
17. COSATI CODES		18. SUBJECT TERMS (Continue on reverse if necessary and identify by block number) GEOSAT, altimeter, water vapor, attenuation			
FIELD	GROUP				SUB. GR.
19. ABSTRACT (Continue on reverse if necessary and identify by block number) <p>→ The GEOSAT Ocean Applications Program (GOAP) is using near-real-time altimeter data to map mesoscale fronts and eddies in the Gulf Stream region. This effort is hampered in part by the fact that atmospheric water vapor can attenuate the altimeter pulse and produce erroneous undulations in the resultant sea surface topography. This report identifies the magnitude and spatial scales associated with water vapor attenuation so that the GOAP analyst can better anticipate the problem at hand.</p> <p>The task is approached by using SEASAT Scanning Multichannel Microwave Radiometer (SMMP) data to define water vapor gradients over the Gulf Stream. The 1978 data clearly reveals that attenuation due to water vapor alone can be 20-40% as large as the 50-100 cm signal characteristic of ocean fronts and eddies. These water vapor gradients also occur on the same scale (100-250 km) as the mesoscale</p>					
20. DISTRIBUTION/AVAILABILITY OF ABSTRACT UNCLASSIFIED/UNLIMITED <input type="checkbox"/> SAME AS RPT. <input checked="" type="checkbox"/> DTIC USERS <input type="checkbox"/>		21. ABSTRACT SECURITY CLASSIFICATION Unclassified			
22a. NAME OF RESPONSIBLE INDIVIDUAL Jeffrey D. Hawkins		22b. TELEPHONE NUMBER (Include Area Code) (601) 688-5270	22c. OFFICE SYMBOL Code 321		

(cont)

UNCLASSIFIED

SECURITY CLASSIFICATION OF THIS PAGE

→ ocean features, ^(illustrating) this fact illustrates the point that the GOAP analyst must interpret individual track information with caution to avoid errors in the analysis.

While A study was also done to simulate what effect these water vapor errors ^{has} would have on objectively contoured topographic fields. The attenuation due to water vapor ~~does have~~ some impact, but it is outweighed by the problems associated with low data density and consequent distortion introduced by the interpolation scheme. The track spacing is thus the dominant problem and will remain so until the GEOSAT Extended Repeat Mission brings about a more appropriate distribution of data. When combined with water vapor data from the Special Sensor Microwave Imager (SSM/I), objective mapping will likely become ~~much~~ more feasible.

A

UNCLASSIFIED

SECURITY CLASSIFICATION OF THIS PAGE